ELSEVIER

Polymer 42 (2001) 8387–8393

polymer

www.elsevier.nl/locate/polymer

Synthesis and solution properties of cylinder brushes derivated by internal domain locking of poly(diblock macromonomer)s

Keiichiro Tsubaki, Koji Ishizu*

Department of Organic Materials and Macromolecules, Graduate School of Science and Engineering, Tokyo Institute of Technology, 2-12-1, Ookayama, Meguro-ku, Tokyo 152-8552, Japan

Received 8 February 2001; received in revised form 13 April 2001; accepted 14 May 2001

Abstract

Poly(diblock macromonomer)s (diblock copolymer brush) were synthesized by free-radical homopolymerizations of vinylbenzyl-terminated poly(α-methylstyrene)-*block*-poly(2-vinylpyridine) (PMS-*block*-P2VP) diblock macromonomer. Dilute-solution properties of such diblock copolymer brushes were investigated by static (SLS) and dynamic light scatterings (DLS) and small-angle X-ray scattering (SAXS). Effective diffusion coefficient D_{eff} for polymer brushes with various aspect ratios showed the almost constant value in the range of polymer concentration $0–5 \times 10^{-3}$ g/cm^3. These results indicated that polymer brushes formed unimolecule structure even in good solvent such as benzene. It was speculated from angular dependence measurements that polymer brushes with large aspect ratios took geometrical anisotropic conformation such as cylinder. Subsequently, the cylinder brushes were derivated by crosslinking of internal P2VP domains of diblock copolymer brushes with 1,4-diiodobutane. These cylinder brushes also formed unimolecular structure in a dilute solution. However, semi-dilute solution properties of cylinder brush show a clear plateau region, which originates from entanglement effect. This entanglement is caused by the thin thickness of PMS shell. © 2001 Published by Elsevier Science Ltd.

Keywords: Diblock copolymer brushes; Unimolecule structure; Cylinder brushes

1. Introduction

Homopolymerization of macromonomers provides the well-defined multi-branched polymers, the so-called poly(macromonomer)s or polymer brushes, which have long side chain at each repeating unit of the backbone. The main chain is extremely extended due to densely grafted side chains. As a result, poly(macromonomer)s are revealed almost worm-like or cylindrical brush conformation at high molecular weight [1–9]. This confirmed that polymer brushes with high degree of polymerization (DP) showed mesophase due to crowded structures [1,10–12], but polymer brushes with extremely high DP showed no mesophase due to worm-like structure [12].

More recently, we have established the synthetic route for rod-like nanopolymers: cross-linking reaction of polystyrene-*block*-poly(4-vinylpyridine) (PS-*block*-P4VP) diblock copolymer (P4VP block, 22 mol%) films exhibiting P4VP cylindrical microdomains with 1,4-dibromobutane in the solid state [13,14]. On the other hand, Liu and co-workers [15] have also reported for the preparation of rod-like nanopolymers by the crosslinking micelles formed by diblock copolymers. However, these preparation methods could not control the major length of rod polymers. To overcome these problems, we synthesized polystyrene-*block*-polyisoprene (S-*b*-I) diblock polymer brushes by free-radical polymerization of (S-*b*-I) diblock macromonomer [16]. Internal PI domains can be locked by the condensation with S_2Cl_2. However, the diblock copolymer brushes possessing high DP could not be obtained due to the chain transfer of propagating polymacromonomer radicals to allyl groups of PI (3,4-addition 50%).

In this article, diblock copolymer brushes with various DP were synthesized by free-radical polymerization of poly(α-methylstyrene)-*block*-poly(2-vinylpyridine) (PMS-*b*-P2VP) diblock macromonomer. Dilute-solution properties of diblock copolymer brushes were studied by static (SLS) and dynamic light scatterings (DLS) and small-angle X-ray scattering (SAXS). Cylinder brushes were derivated by crosslinking internal P2VP domains of diblock copolymer brushes with dihalide. We discussed in detail on the molecular conformation of diblock copolymer and cylinder brushes in not only dilute but also semi-dilute solutions from LS and rheological measurements.

* Corresponding author. Tel.: +81-3-5734-3550; fax: +81-3-5734-2888.
E-mail address: ktsubaki@polymer.titech.ac.jp (K. Ishizu).

0032-3861/01/$ - see front matter © 2001 Published by Elsevier Science Ltd.
PII: S0032-3861(01)00347-0

2. Experimental

2.1. Synthesis and characterization of diblock macromonomers

Vinylbenzyl-terminated (PMS-*block*-P2VP) diblock macromonomers (MSV) were synthesized by the living anionic polymerization technique of coupling reaction of corresponding diblock lithium with a small-excess amount of *p*-chloromethylstyrene (CMS) in a tetrahydrofuran (THF). Diblock macromonomers were recovered by the precipitation from THF/*n*-hexane system. The number-average molecular weights (M_n) were determined by vapor pressure osmometer (VPO; CORONA 117) in benzene. The molecular weight distribution (M_w/M_n) was determined by gel permeation chromatography (GPC; Tosoh high-speed liquid chromatography HLC-8020, TSK gel G2000H_{XL} and two GMH_{XL} columns, in series) using THF as the eluent at 38°C. Details of the synthesis and characterization of diblock macromonomers were given elsewhere [17,18]. Characteristics of diblock macromonomers are listed in Table 1.

2.2. Synthesis of diblock copolymer brushes

Free-radical polymerizations of diblock macromonomers were carried out in benzene at 60°C using 2,2′-azobisisobutyronitrile (AIBN) as an initiator in a sealed glass ampoule under high vacuum. After polymerization, the solution was poured into an excess of hexane. Unreacted MSV was removed from the polymerization products by the precipitation fractionation with a benzene–hexane system. Subsequently, the diblock copolymer brush obtained was fractionated stepwise by precipitation fractionation to perform narrow molecular weight distribution.

A combination of GPC with light scattering (LS) detector is very useful for measuring the weight-average molecular weight (M_w) and molecular weight distribution of branched polymers such as polymer brushes, since one does not need any isolation procedures to remove unreacted diblock macromonomers. GPC measurements were carried out with a Tosoh high-speed liquid chromatography HLC-8120 equipped with a low-angle laser light scattering (LALLS) detector, LS-8 (He–Ne laser with a detection angle of 5°) and refractive index (RI), which was operated with TSK gel G2000H_{XL} and two GMH_{XL} columns, in series using THF as the eluent at 40°C. The conversion of diblock copolymer brushes was determined by the change in the ratio of the peak area of the diblock polymer brush produced to the total peak area of the polymerization product in GPC charts. The details concerning the calculation method for M_w have been given elsewhere [19].

Table 1
Characteristics of diblock macromonomers

No.	$\bar{M}_n$ [a]	$\bar{M}_n/\bar{M}_w$ [b]	PMS block[c] (mol%)	Functionality[c]
MSV1	2700	1.19	77	0.92
MSV2	2800	1.31	76	0.90
MSV3	2900	1.20	67	0.90
MSV4	7100	1.35	75	0.91

[a] Determined by VPO.
[b] Determined by GPC.
[c] Determined by ^{1}H-NMR.

2.3. Dilute-solution properties of diblock copolymer brushes

The M_w, the second virial coefficient (A_2) and the radius of gyration (R_g) of diblock copolymer brushes with high DP were determined by static light scattering (SLS; Photal TMLS-6000HL: Otsuka Electronics, $\lambda_0 = 632.8$ nm) in benzene ($\eta = 0.654$ cp, $n_D = 1.498$) at 25°C in the Berry mode. The Berry treatment is used widely in the characterization of branched structures, such as star polymers [20]. The scattering angle was in the range 30–150°. The solutions were prepared in the concentration range 0.32–5.10 mg/ml. The RI increment d*n*/d*c* of each sample was measured with a differential refractometer (Photal DRM-1021: Otsuka Electronics). Sample solutions were filtered through membrane filters with a nominal pore of 0.2 μm just before measurement.

Since R_g of low molecular weight diblock polymer brushes is very small, it is impossible to evaluate R_g from SLS. Then R_g was determined by SAXS. The SAXS intensity distribution $I(\mathbf{q})$ was measured with rotating-anode X-ray generator (Rigaku Denki Rotaflex RTP 300 RC) operated at 40 kV and 100 mA. The X-ray source was monochromatized Cu Kα ($\lambda = 1.54$ Å) radiation. In the measurement of a benzene solution (0.5–5.0 wt%) of the sample, we used the cell sandwiched between mica plates as a holder vessel. The background correction was carried out using polyethylene film. The value of R_g is estimated by Guinier's method from the following equation [21]:

$$\ln I(\mathbf{q}) = \text{const} - (1/3)(R_g^2)\mathbf{q}^2 \quad (1)$$

where $\mathbf{q}$ is the scattering vector. The value of cross-sectional radius of gyration ($R_{g,c}$) is estimated from the following equation [22]:

$$\ln [I(\mathbf{q})\mathbf{q}] = \text{const} - (1/2)(R_{g,c}^2)\mathbf{q}^2 \quad (2)$$

The diffusion coefficient (D_0) was determined by the extrapolation to zero concentration on dynamic light scattering (DLS; Otsuka Electronics) data with cumulant method at 25°C in 0.35–5.20 mg/ml benzene solution. The scattering angle was in the range 30–150°.

Geometrical anisotropy of diblock copolymer brushes was discussed by means of the angular dependence $\Gamma_e\mathbf{q}^{-2}$ vs. $\mathbf{q}$ of effective diffusion coefficient ($D_{eff} = \Gamma_e\mathbf{q}^{-2}$; $\Gamma_e\mathbf{q}^{-2}$ vs. $\mathbf{q}$), where Γ_e and $\mathbf{q}$ indicate the decay rates (first cumulant) and scattering vector, respectively.

2.4. Crosslinking internal P2VP domains of diblock copolymer brushes

In order to obtain cylinder brushes, we carried out the crosslinking reaction of diblock copolymer brushes (0.05–0.1 wt%) with 1,4-diiodobutane (feed amounts = 50 mol% based on P2VP units) in THF for 3 days. Degree of quaternization (DQ) of cylinder brushes was determined by Volhard's titration. Dilute-solution properties of cylinder brushes were also investigated by SLS and DLS. Rheological measurements of diblock polymer brushes and cylinder brushes (20 wt% *o*-xylene solutions) were performed to make clear semi-dilute solution properties on ARES (Rheometric Scientific) using cone-plate geometry ($\phi = 25$ mm, cone angle = 0.04 rad, frequency range = 1–200 Hz) at 25°C.

3. Results and discussion

3.1. Synthesis of diblock copolymer brushes

Vinylbenzyl-terminated P2VP macromonomer was synthesized previously by Takaki et al. [23]. They carried out the reaction of living P2VP anion with *p*-CMS (small excess against living ends) and prepared monodisperse macromonomer with high functionality (>96%). It was confirmed that the carbanions of living P2VP do not attack the vinyl group but react only with chloromethyl group of *p*-CMS. In this article, (PMS-*b*-P2VP) diblock macromonomers were synthesized by using the similar method described above. Typical GPC profiles of MSV2 diblock macromonomer are shown in Fig. 1. GPC profile shows unimodal pattern with relatively narrow molecular weight distribution ($M_w/M_n = 1.31$). The functionalities of diblock macromonomers are more than 0.9.

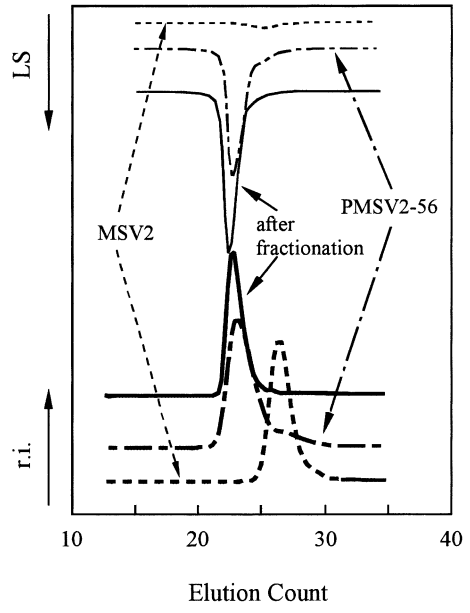

Fig. 1. GPC profiles of MSV diblock macromonomer, PMSV2-56, and diblock copolymer brush.

Free-radical polymerizations of diblock macromonomers were carried out in benzene using AIBN as the initiation at 60°C. Polymerization conditions and results are listed in Table 2. Fig. 1 shows typical GPC profiles of PMSV2-56 taken with RI and LS detectors. The GPC distribution of PMSV2-56 is bimodal. It is seen that the polymerization product is the mixture of copolymer brush and a small amount of unreacted diblock macromonomer. The value of M_w, M_w/M_n and conversion are estimated from the GPC chart. These physical values are also listed in Table 2. The molecular weight distributions of copolymer brushes became broad with an increment of DP (M_w/M_n = 1.18–1.28). The DP of diblock copolymer brushes were controlled by the initial concentration of macromonomer $[M]_0$. The conversions reached more than 80% in contrast with the results for (PS-*block*-PI) copolymer brushes (ca. 18.5–40.3%) [16]. Polymerization products were fractionated by precipitation method (benzene/hexane system) to narrow the molecular weight distribution of copolymer brushes.

3.2. Solution properties of diblock polymer brushes

M_w and R_g of diblock copolymer brushes were derived from Berry plot in benzene. Typical Berry plot of diblock copolymer brush PMSV1-406 is shown in Fig. 2. R_g of copolymer brushes (PMSV2-19, PMSV2-24, PMSV2-38, and PMSV4-30) was determined by Guinier's plots on SAXS due to their small DP. On the other hand, $R_{g,c}$ of diblock copolymer brushes was determined by cross-sectional Guinier's plots on SAXS. Typical Guinier's and cross-sectional Guinier's plots for PMSV2-56 are shown in Figs. 3 and 4, respectively, as functions of polymer concentrations. The values of R_g and $R_{g,c}$ were estimated from the corresponding slope of both plots at the small-angle region

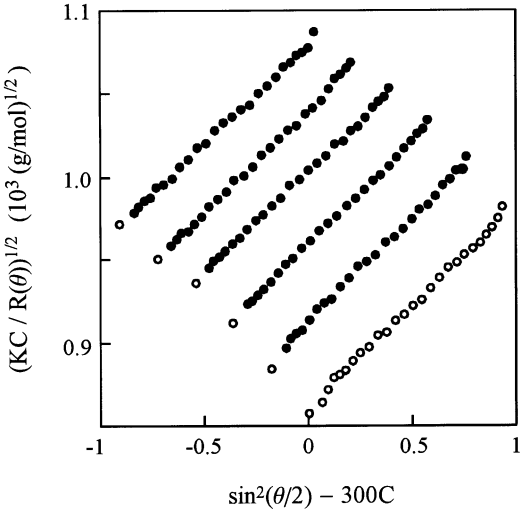

Fig. 2. Berry's plot of diblock copolymer brush PMSV1-406 in benzene.

Table 2
Polymerization condition and results of MSV1, polymerized in benzene initiated by AIBN at 60°C for 100 h

No	Feed		Polymer brush			
	[M] (mol/l)	$[I]\times10^2$ (mol/l)	$\bar{M}_w\times10^{-5}$ [a]	$\bar{M}_w/\bar{M}_n$ [b]	Conversion[b] (%)	DP[a]
PMSV1-54	0.159	0.850	1.73	1.18	90.2	54
PMSV1-94	0.185	0.750	3.01	1.20	90.3	94
PMSV1-113	0.205	0.667	3.62	1.26	80.8	113
PMSV1-131	0.220	0.600	4.19	1.28	81.3	131

[a] Determined by LALLS–GPC.
[b] Determined by GPC.

($\mathbf{q}R < 1$), respectively. These physical values are listed in Table 3. Fig. 5 shows the relationship between $R_{g,c}$ and DP for PMSV1, PMSV2, and PMSV4 series. It is found that the values of $R_{g,c}$ are almost constant in each series. This result means that copolymer brushes exhibit the same radius regardless of aspect ratios.

In order to discuss the geometrical anisotropy and intermolecular interaction, we determined the translational diffusion coefficient (D_0) of diblock polymer brushes. In general, the mutual diffusion coefficient $D(C)$ is defined as $D(C) \equiv \Gamma_e \mathbf{q}^{-2}_{\theta\to0}$, where θ is the scattering angle. Angular dependence of $\Gamma_e\mathbf{q}^{-2}$ ($\mathbf{q}R_h < 1$) for PMSV1-406, PMSV3-21, and PMSV4-74 is shown in Fig. 6. In the case of spherical shape, it is well known that the slope of line ($\Gamma_e\mathbf{q}^{-2}$ vs. $\mathbf{q}$: $\mathbf{q}R_h < 1$) shows zero. It is found that the observed data on diblock copolymer brush PMSV3-21 are fitted on the almost flat line. This copolymer brush is composed of short backbone (DP = 21). It seems therefore that the PMSV3-21 takes the shape of sphere or ellipsoid in the dilute solution. On the other hand, the copolymer brush PMSV1-406 and PMSV4-74 shows angular dependence. These diblock copolymer brushes are composed of long backbone length (DP = 406 and 74). It is concluded that the shape of polymer brush changes from sphere (or ellipsoid) to rod-like cylinder in the dilute solution with increasing the DP of copolymer brush.

Fig. 7 shows the relationship between translational diffusion coefficient $D(C)$ and polymer concentration C for PMSV1-158, PMSV1-406, and PMSV1-1017. Each $D(C)$ has an almost constant value in the range of $0–5\times10^{-3}$ g/cm^3 polymer concentration for all of the samples. This suggests that these diblock copolymer brushes form unimolecule structure in such polymer concentrations. Similar tendencies were also observed in hetero-arm copolymer brushes [24] and highly branched stars [25,26]. The translational diffusion coefficient D_0 can be estimated by extrapolation of polymer concentration C to zero. The values of D_0 and R_h are listed in Table 4. R_h is defined as Stokes–Einstein's equation: $R_h = kT/6\pi\eta_0 D_0$, where k, T, and η_0 indicate Boltzmann coefficient, absolute temperature, and viscosity of solvent, respectively. It is found that D_0 decreases with increasing DP in the same series. This is a reasonable result.

3.3. Dilute and semi-dilute solution properties of cylinder brushes

In order to obtain the cylinder brushes, we carried out the

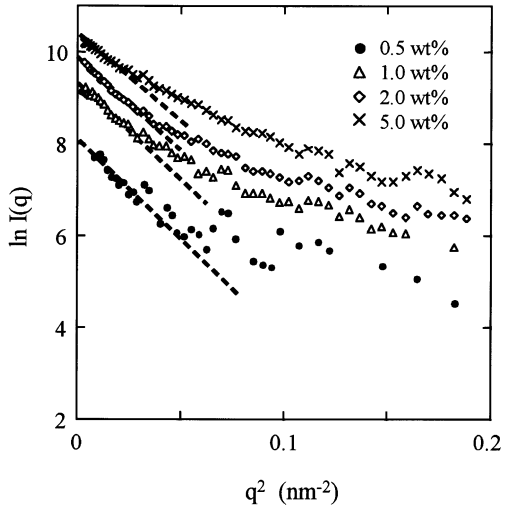

Fig. 3. Typical Guinier's plots of PMSV2-56 (0.5–5.0 wt%).

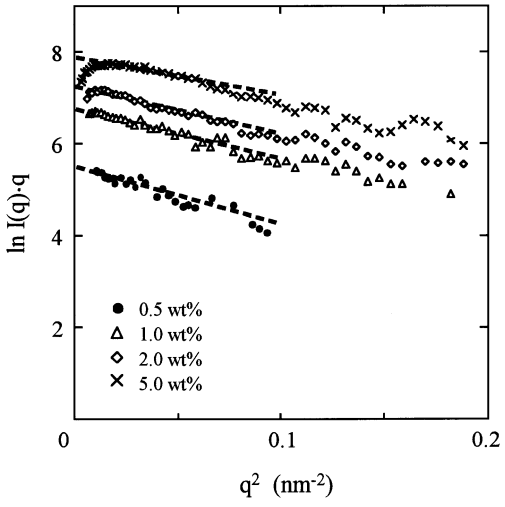

Fig. 4. Typical cross-sectional Guinier's plots of PMSV2-56 (0.5–5.0 wt%).

Table 3
Dilute-solution properties of diblock polymer brushes in benzene

No.	$\bar{M}_w \times 10^{-5}$ [a]	DP	R_g [b] (nm)	$R_{g,c}$ [c]
PMSV2-19	0.68	19	6.9[d]	3.2
PMSV2-24	0.86	24	7.6[d]	3.3
PMSV2-38	1.37	38	8.6[d]	3.3
PMSV2-53	1.91	53	12.1	3.3
PMSV2-56	2.02	56	12.5	3.3
PMSV4-30	2.88	30	8.2[d]	5.1
PMSV4-76	7.30	76	13.2	5.0
PMSV4-115	11.0[b]	115	23.1	5.4
PMSV1-158	5.07[b]	158	16.0	3.2
PMSV1-410	13.1[b]	410	27.0	3.5
PMSV1-1017	32.5[b]	1017	41.2	3.6

[a] Determined by LALLS–GPC.
[c] Determined by SLS.
[d] Caluculated by cross-sectional Guinier's plot.
[b] Caluculated by Guinier's plot.

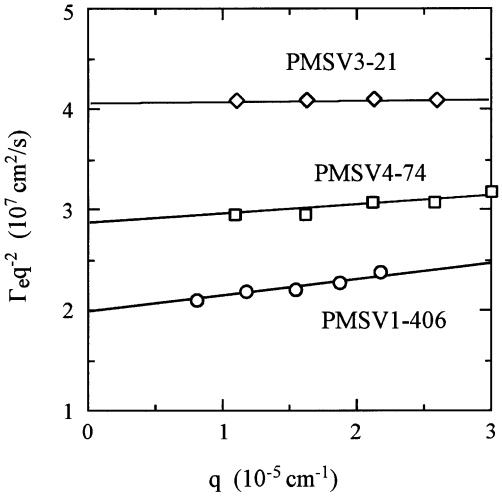

Fig. 6. Angular dependence $\Gamma_e \mathbf{q}^{-2}$ vs. $\mathbf{q}$ for diblock copolymer brush PMSV1-406, PMSV3-21, and PMSV4-74.

crosslinking reaction of internal P2VP domain of diblock copolymer brushes with 1,4-diiodobutane in dilute-solution. DQ of cylinder brushes was estimated by Volhard's titration in benzene/water. The DQ of PMSV1-406C and PMSV3-21C was 38.1 and 43.6 mol%, respectively. Therefore, quaternized P2VP domains were regarded as hydrophilic domains. Dilute-solution properties of cylinder brushes were also investigated by the SLS and DLS measurements. Fig. 8 shows the relationship between $D(C)$ and C for PMSV1-406, PMSV1-406C, PMSV3-21, and PMSV3-21C. Each $D(C)$ for cylinder brushes PMSV1-406C and PMSV3-21C shows a constant value in dilute-solution region. This suggests that cylinder brushes form unimolecular structure in a dilute solution such as copolymer brushes. Furthermore, it is noticed that the observed values of $D(C)$ for cylinder brushes (PMSV1-406C and PMSV3-21C) are somewhat smaller than those for corresponding diblock copolymer brushes. That is to say, the hydrodynamic radius R_h of cylinder brushes increases compared to that of corresponding copolymer brushes. The internal P2VP domains are converted into hydrophilic gel due to crosslinking reaction (quaternization). Because of its not only high segment density but also hydrophilic nature, the cylinder brush is drained only at periphery around cylinders. Similar behavior was also observed in microgel [27]. On the other hand, radius of gyration R_g of cylinder brushes are also somewhat smaller than those for corresponding diblock copolymer brushes due to the compact nature by internal domain locking.

To investigate the viscoelasticity of diblock copolymer brush and cylinder brush, we carried out the rheological measurement in semi-dilute solution. Rheological properties

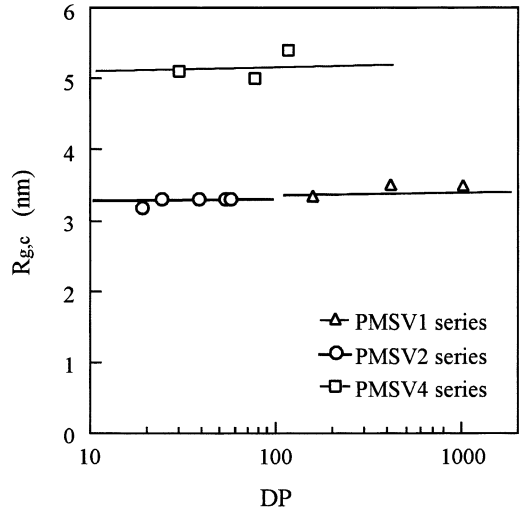

Fig. 5. The relationship between cross-sectional radius $R_{g,c}$ and DP for PMSV1, PMSV2, and PMSV4 series.

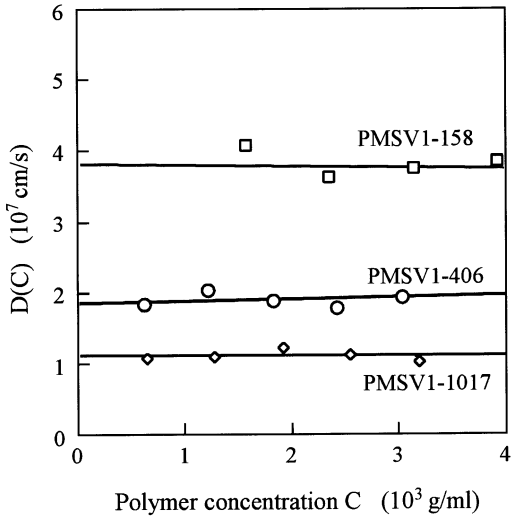

Fig. 7. Plot of translational diffusion coefficient $D(C)$ of diblock copolymer brush PMSV1-1017, PMSV1-406, and PMSV1-158 against polymer concentration.

Table 4
Dilute-solution properties of cylinder brushes and diblock polymer brushes

No.	$\bar{M}_w \times 10^{-5}$ [a]	$A_2 \times 10^5$ (cm^3 mol/g^2)[a]	R_g[a] (nm)	$D_0 \times 10^{7}$[b] (cm^2/s)	R_h[b] (nm)
PMSV1-158	5.07	9.25	16.0	4.03	9.0
PMSV1-1017	32.5	0.99	41.2	1.08	33.8
PMSV1-406	12.9	2.84	31.0	1.91	19.1
PMSV1-406C[c]	14.3	0.99	28.3	1.69	21.4
PMSV3-21	0.63	33.8	15.1	3.99	9.2
PMSV3-21C[c]	0.76	26.6	14.7	3.69	9.8

[a] Determined by SLS.
[b] Determined by DLS (Cumulant Method).
[c] Cylinder brush.

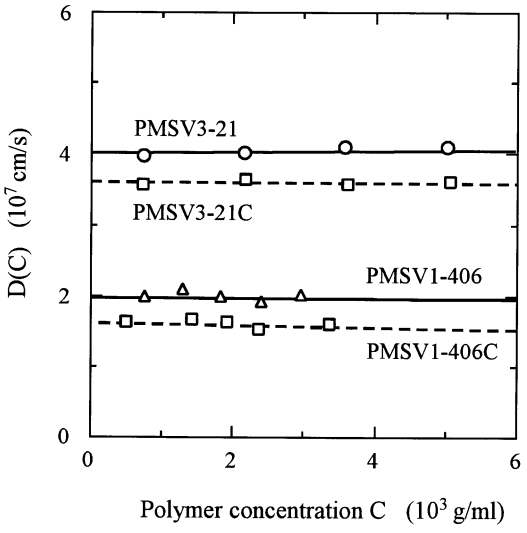

Fig. 8. Plot of translational diffusion coefficient $D(C)$ of cylinder brush (PMSV1-406C, PMSV3-21C) and corresponding diblock copolymer brush (PMSV1-406, PMSV3-21) against polymer concentration C.

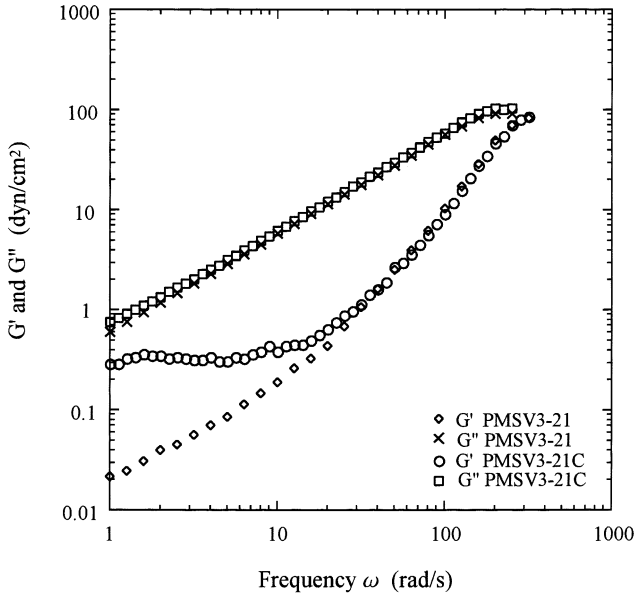

Fig. 9. The relationship between dynamic shear moduli (storage modulus G' and loss modulus G'') and angular frequency ω for PMSV3-21 and PMSV3-21C in *o*-xylene (20 wt%).

of poly(PS macromonomer)s (PS type polymer brushes) were investigated previously by Tsukahara and co-workers [28]. They discussed bulk properties of multi-branched polystyrenes by the master curve of the storage dynamic shear modulus G'. Consequently, it was indicated that the intermolecular chain entanglement might be strongly restricted in the poly(macromonomer) (polymer brush) system due to the multi-branched structure of high branch density. Fig. 9 shows the relationship between dynamic shear moduli (storage modulus G' and loss modulus G'') and angular frequency ω for PMSV3-21 and PMSV3-21C in *o*-xylene (20 wt%). The observed G' and G'' for diblock copolymer brush PMSV3-21 are fitted on the same curve. However, G' for cylinder brush PMSV3-21C shows a clear plateau region at $\omega = 10^0 - 2 \times 10^1$ (rad/s). In general, such slow relaxation mode originates from entanglement effects. The P2VP block content of PMSV3 series is 33 mol%. So, the cylindrical core of PMSV3-21 brush stabilizes sterically with relatively thin thickness of PMS shell parts. It seems that the cylinder brushes lead to intermolecular interaction among crosslinked cylindrical cores in semi-dilute solution. This fusion behavior was also observed in core-shell polymer microspheres composed of isotropic geometrical structure [29].

Such rheological behaviors will be made clear by the measurements as a function of PMS shell thickness. Further work on the rheological behaviors of cylinder brushes is in progress.

References

[1] Wintermantel M, Fischer K, Gerle M, Ries R, Schmidt M, Kajiwara K, Urakawa H, Wataoka I. Angew Chem Int Ed Engl 1995;107:1606.
[2] Wintermantel M, Gerle M, Fischer K, Schmidt M, Wataoka I, Urakawa H, Kajiwara K, Tsukahara Y. Macromolecules 1996;29:978.
[3] Wintermantel M, Schmidt M, Tsukahara Y, Kajiwara K, Kohjiya S. Macromol Rapid Commun 1994;15:279.
[4] Tsukahara Y, Kohjiya S, Tsutsumi K, Okamoto Y. Macromolecules 1994;27:1662.
[5] Nemoto N, Nagai M, Koike A, Okada S. Macromolecules 1995;28:3854.
[6] Wataoka I, Urakawa H, Kajiwara K, Schmidt M, Wintermantel M. Polym Int 1997;44:365.
[7] Terao K, Nakamura Y, Norisuye T. Macromolecules 1999;32:711.

[8] Kawaguchi S, Imai G, Suzuki J, Miyahara A, Kitano T, Ito K. Polymer 1997;38:2885.
[9] Kawaguchi S, Matsumoto H, Iriany, Ito K. Polym Prepr Jpn 1998;47:1694.
[10] Tsukahara Y, Ohta Y, Senoo K. Polym Prepr Jpn 1995;43:121.
[11] Tsukahara Y, Ohta Y, Senoo K. Polymer 1995;36:3413.
[12] Tsukahara Y, Miyata M, Senoo K, Yoshimoto N, Kaeriyama K. Polym Adv Technol 2000;11:210.
[13] Ishizu K, Ikemoto T, Ichimura A. Seni Gakkaishi 1998;54:301.
[14] Ishizu K, Ikemoto T, Ichimura A. Polymer 1999;40:3147.
[15] Tao J, Stewart S, Liu G, Yang M. Macromolecules 1997;30:2738.
[16] Ishizu K, Tsubaki K, Ono T. Polymer 1997;39:2935.
[17] Ishizu K, Kuwahara K. Polymer 1994;35:4907.
[18] Ishizu K, Shimomura K, Fukutomi T. J Polym Sci, Polym Chem Ed 1991;29:923.
[19] Ishizu K, Shimomura K, Saito R, Fukutomi T. J Polym Sci, Polym Chem Ed 1991;29:607.
[20] Katime I, Quintana JR. In: Booth C, Price C, editors. Comprehensive polymer science, vol. 1. Oxford: Pergamon Press, 1989. Chap. 5.
[21] Guinier A. Ann Phys 1939;12:161.
[22] Guinier A, Fournet G. Small-angle scattering of X-rays. New York: Wiley, 1955.
[23] Takaki M, Asami R, Tanaka S, Hayashi H. Macromolecules 1986;19:2900.
[24] Tsubaki K, Kobayashi H, Sato J, Ishizu KJ. Colloid Interf Sci (submitted for publication).
[25] Ishizu K. Prog Polym Sci 1998;23:1383.
[26] Ishizu K, Uchida S. Prog Polym Sci 1999;24:1439.
[27] Mossmer S, Spatz JP, Moller M, Aberle T, Schmidt J, Barchard W. Macromolecules 2000;33:4791.
[28] Namba S, Tsukahara Y, Kaeriyama K, Okamoto K, Takahashi M. Polymer 2000;41:5165.
[29] Ishizu K, Naruse F, Saito R. Polymer 1994;35:2329.